Proc. of SPIE Vol. 1690, Design of Optical Instruments, ed. D M Aikens, V L Genberg, G C Krumweide, M J Thomas (Sep 1992) Copyright SPIE

Recent developments with the Mars Observer Camera graphite/epoxy structure

Arthur R. Telkamp

OCA Applied Optics
7421 Orangewood Avenue, Garden Grove, California 92641

ABSTRACT

This paper discusses the significant events that have occurred in the past two years with the Mars Observer Camera (MOC) graphite/epoxy structure. Topics were chosen that highlight information that may be of interest to the industry, and updates the progress reported in the previous similar paper entitled "Design considerations for composite materials used in the Mars Observer Camera", presented at the April 1990, Orlando, SPIE conference on Advances in Optical Structure Systems. The topics discussed herein are:

1. The implementation of thermal blankets, shields, and thermal control paints to limit solar absorption while controlling stray light.
2. Vibration testing of Flight Unit #1. Corrective repairs were made after sustaining damage during the first vibration test. The subsequent vibration test technique was refined and the unit passed successfully.
3. Thermal expansion testing -- technique and test results for both flight units. Flight Unit #1 behaves different from Flight Unit #2.
4. The results of thermal-vac testing Flight Unit #1. Although the temperature profiles were as predicted, the thermally-induced focus displacements were not. However, the thermal environment does not upset the image quality.

1. INTRODUCTION

The Mars Observer Camera (MOC) is one of several instruments aboard the Mars Observer Spacecraft, whose mission is to geologically and climatologically map the Martian surface and atmosphere over a period of one Martian year (687 Earth-days). Although the Mars Observer Spacecraft is scheduled to be launched as early as 16 September 1992 (but no later than 6 October 1992), mapping operations will not begin until December 1993 because of an eleven-month interplanetary cruise time and an additional four months to establish the spacecraft's proper polar orbit around Mars. Mapping operations are now scheduled to take place from 16 December 1993 to 3 November 1995 at a mean altitude of 390 Km.[1]

The MOC is the only instrument that will return visual images of the surface and atmosphere of Mars, and comprises three separate optical systems: a narrow-angle camera and two wide-angle cameras. The Narrow-Angle camera will return high resolution imagery of the surface of Mars with its 3.5-meter focal length, f/10 Ritchey-Chretien telescope. The wide-angle cameras will return limb-to-limb imagery of the Martian surface and atmosphere with their ±70° fields-of-view. The Red Wide-Angle camera images in the 575 to 625 nm band, and the Blue Wide-Angle camera images in the 400 to 450 nm band.

This paper discusses major events that have occurred in the past two years with the MOC graphite/epoxy structure. In order to clearly convey the details of these topics, a brief description of the MOC structure is necessary. The remainder of this section describes the Flight Unit structure; however, to gain a clear understanding of the design details and background, "Design considerations for composite materials used in the Mars Observer Camera"[2] is recommended reading.

The MOC structure basically comprises three subassemblies: The Main Body Structural Assembly (MBSA), the Secondary Mirror Support Assembly (SMSA), and the Wide-Angle Support Assembly (WASA). Figure 1 shows a cutaway view of the MOC Flight Model and the relationships of these subassemblies. Sans electronics boards, the MOC optics and structure weighs approximately 20 pounds.

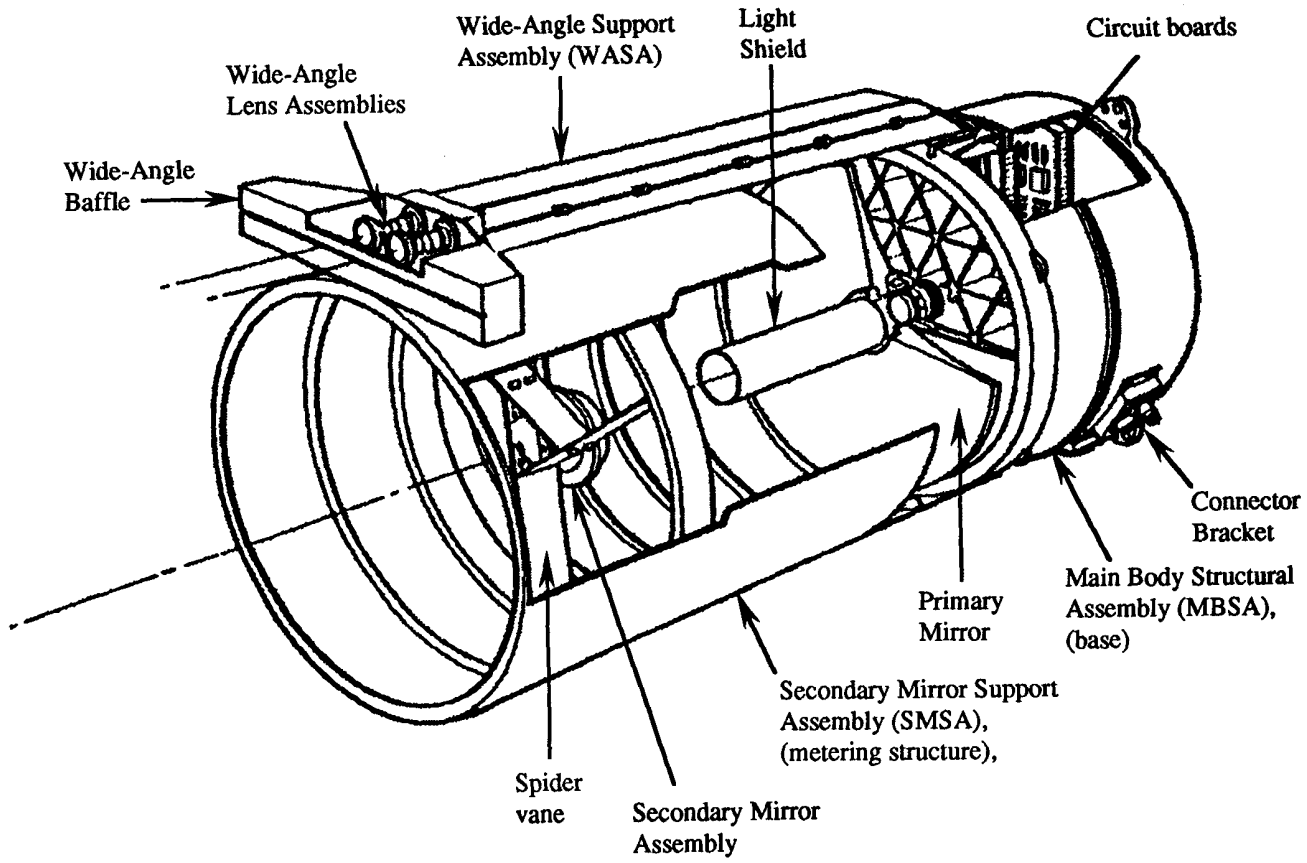

Figure 1. MOC Flight Unit cutaway view.

The MBSA is the base of the Narrow-Angle telescope and consists of two parts. The upper portion of the MBSA is made entirely from graphite/epoxy except for an Invar mounting ring at the center of the upper surface of the MBSA to provide attachment of the Primary Mirror Assembly (which, in turn, supports the Narrow-Angle Focal Plane Assembly), and six Invar fittings at the upper periphery of the MBSA that mate with similar fittings at the lower periphery of the metering structure. The lower portion of the MBSA is a 4-inch long aluminum cylinder that supports three aluminum-honeycomb-core electronics boards and facilitates attachment to the aluminum nadir panel. This aluminum cylinder is called the Base Radiator because it is the primary heat rejector for the electronics boards.

A cylindrical assembly consisting of an "egg crate" lattice structure constructed from pre-cured graphite/epoxy laminates (ribs), onto which a top and bottom facesheet is bonded, provides a rigid platform for which to mount the Primary Mirror Assembly. The facesheets and ribs are made from P75S/ERL1962 graphite/epoxy. Transition from this cylindrical portion of the MBSA to the Base Radiator was accomplished via the use of a T300/934 graphite/epoxy cone section which acts as a thermal flexure between the graphite/epoxy MOC structure and the aluminum Base Radiator. The interface between the low-CTE graphite/epoxy skirt and the high-CTE aluminum base is accommodated by 34 finger flexures around the periphery.

The MOC umbilical supplies the camera with nitrogen purge gas and electrical power, and relays data from the MOC to the spacecraft and vice versa. The umbilical connects to the MOC at the aluminum Connector Bracket which is mounted to the side of the aluminum Base Radiator.

The SMSA, otherwise known as the metering structure, accurately separates the secondary mirror from the primary mirror, and provides an outer baffle for the Narrow-Angle telescope. The SMSA is made entirely of P75S/ERL1962 graphite/epoxy except for the six Invar fittings at its lower periphery and three Invar fittings at the center of its spider assembly that allow

attachment of the Secondary Mirror Assembly. The SMSA is basically a 15.5-inch diameter by 25.7-inch long by .020-inch wall thickness tube with 11 stiffening rings along its length. The stiffening rings also act as baffle vanes. At about two-thirds the height of this tube are the spider vanes that hold the Secondary Mirror Assembly. There is a stiffening ring bonded to the top and bottom of the spider vane assembly, and the volume between the rings is closed-out by an inner wall (thus becoming the spider stiffening annulus). The spider vane arrangement was designed such that any thermal expansion or contraction along the length of the vanes will result in only a rotation of the secondary mirror. (Cassegrain telescopes are very sensitive to despace, decenter, and tilt of the secondary mirror, but not to rotation).

The WASA supports the Wide-Angle Lens Assemblies and the Wide-Angle Baffle. It is basically a hollow, 2-inch square tube made of P75S/ERL1962 graphite/epoxy; the lower end of which attaches to the MBSA via a single-point flexure, and the upper end attaches to the SMSA at the height of the spider via a two-point flexure. The Wide-Angle Lens Assemblies attach to the titanium "Transition Bracket" At the upper end of the WASA. The Transition Bracket accommodates the transition of the relatively high-CTE titanium lens housings to the low-CTE graphite/epoxy WASA tube while maintaining boresight to the Narrow-Angle telescope over temperature. The Wide-Angle Focal Plane Assemblies are housed in the Transition Bracket. The Wide-Angle Baffle is made entirely of P75S/ERL1962 graphite/epoxy and attaches to the Transition Bracket.

2. SOLAR RADIATION/STRAY LIGHT CONTROL

The external surfaces of the MOC, as well as a majority of the spacecraft, is covered with multi-layer insulation (MLI) to reduce large thermal excursions caused by solar heating and the extreme cold of deep space. This MLI, like most types, consists of several layers of highly reflective Mylar. So, naturally, there were no plans to blanket the internal area of the metering structure, because although this would further reduce thermal excursions, it would become a formidable contributor to stray light. Instead, the internal surfaces of the metering structure were painted with MH21S/LO. MH21S/LO is a black thermal control paint manufactured by the Illinois Institute of Technology Research Institute (IITRI). Its solar absorptance is very high (0.98 to 0.99) which makes it good for reducing stray light; however, it causes the metering structure to absorb solar radiation and become too hot during cruise maneuvers.

2.1. Solar radiation problems

Thermal analysis has since shown that even assuming bare P75S/ERL1962 (with an emissivity of 0.86), the metering structure will attain a temperature of 115°C at steady state when the sun is 35° from the optical axis (55° angle of incidence on the metering structure tube). The Mars Observer Project has assured a "30° solar exclusion zone" for all instruments facing normal to the nadir panel, which means the sun will always be greater than 30° from the MOC optical axis during cruise. Unfortunately, this also means that solar radiation can have an angle of incidence on the internal surface of the metering structure tube anywhere from 60° to just shy of 0° for extended periods. Using the relationship, $E = \sigma T^4$, we can generate the equation,

$$T_\theta = \left[(115+273)^4 \frac{\cos(90°-\theta)}{\cos(90°-35°)} \right]^{\frac{1}{4}} - 273$$

to estimate the maximum steady state temperature of the tube, T_θ (in °C), when the sun is at an angle, θ, from the optical axis (assuming a surface emissivity of 0.86). From this, we can see that the tube can reach nearly 173°C. The graphite/epoxy structure can not be exposed to temperatures greater than 100°C because this is the temperature at which the bond joints were cured. Exceeding this temperature may exceed the moisture-saturated (worst case) glass transition temperature (T_g) of the bond joints and allow them to soften and possibly take on a new set.

To make matters worse, the "30° solar exclusion zone" does not include occasions when the spacecraft must make trajectory correction maneuvers, and the sun could slew within the exclusion zone at a rate of 0.2°/sec. If this occurs, solar radiation will reflect off the primary mirror, and at approximately 22° from axis, come to a sharp focus on the spider stiffening annulus (see Figure 2.1). The resulting irradiance is 4.6 W/cm^2, which is 34 times times the solar constant. Therefore, assuming the solar constant can generate a temperature of 173°C on the graphite/epoxy tube, the temperature in the vicinity of focus (at steady state) can reach $34^{(1/4)}(173+273)-273 = 804$°C.

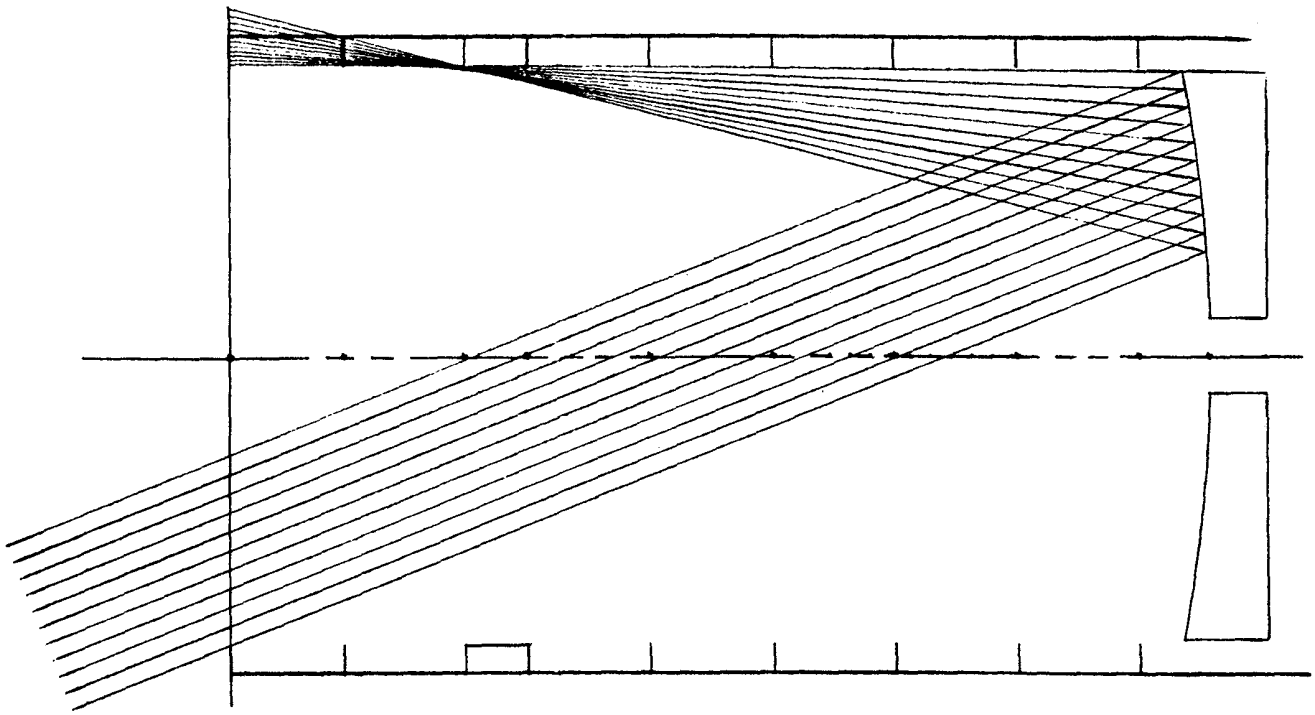

Figure 2.1. Concentration of solar radiation on the spider stiffening annulus at 22° from axis.

2.2. Solar radiation solutions

To reduce the solar absorptance of the small external areas not already covered by MLI (the outer stiffening/baffle ring of the metering structure and the front surface of the Wide-Angle Baffle), these areas were painted with S13G/LO-41. S13G/LO-41 is a white thermal control paint manufactured by IITRI, and has a solar absorptance of 0.15 and a normal emittance of approximately 0.90. Like MH21S/LO, it is siloxane-based so it has a low CTE and is very elastic so it will not stress or deform its graphite/epoxy substrate with temperature.

To protect the interior of the metering structure from direct solar radiation, yet limit the stray light impact, special MLI was made. This MLI is made up of the typical highly reflective layers, except it has a carbon-impregnated Kapton outer layer. The carbon-impregnated Kapton is very black, but with a slight semi-gloss. This black outer layer limits the stray light, and in so doing, absorbs solar radiation, but the sub-layers insulate the heat from the graphite/epoxy metering structure. Individual blankets were made from this special MLI and fitted against the metering tube, between the stiffening/baffle rings. They are held in place by their own hoop spring force. Each blanket covers the wall area between stiffening/baffle rings and the outward facing surface of each lower adjacent ring. Blankets were also fitted and sewn over each spider vane as well.

To protect the spider stiffening annulus from the concentrated solar radiation, three sections of thin aluminum shielding designed to fit between the spider vanes, cover the wall and lower ring of the spider stiffening annulus. The aluminum shields were painted with MH11Z, which is a black, high-temperature, water-based paint manufactured by the Jet Propulsion Laboratory (JPL).

2.3 Stray light issues

Because the black Kapton has a slight semi-gloss while MH21S/LO is a matte black, it was feared that the black Kapton blanketing would cause some measurable increase in stray light. With the help of Bob Breault, of Breault Research Organization, Point Source Transmission (PST) tests were performed to check this.

In the process of setting up to measure the PST, we noticed the direct path scatter from the inside surface of the Light Shield was very bright and would certainly overwhelm any slight difference between the two types of metering structure surfaces. The Light Shield tube was made from T300/934 graphite/epoxy, bonded to an Invar base; painted inside and outside with Chemglaze Z-306. The Light Shield design is shown in Figure 2.2a. Of course, the Light Shield design had to be changed, but to be able to continue our PST testing of the metering structure surfaces, we lined the the internal surface of the Light Shield with black velvet. To our surprise, there was absolutely no difference between the two types of metering structure surfaces; perhaps attributable to the otherwise good geometry of the Light Shield.

The Light shield design has since been changed to that shown in Figure 2.2b. It is made entirely of 6061-T6511 aluminum and coated with Martin Marietta's Optical Black (Martin Black). Note that baffle vanes were added for good measure, and where no vanes could be added, the surface was threaded.

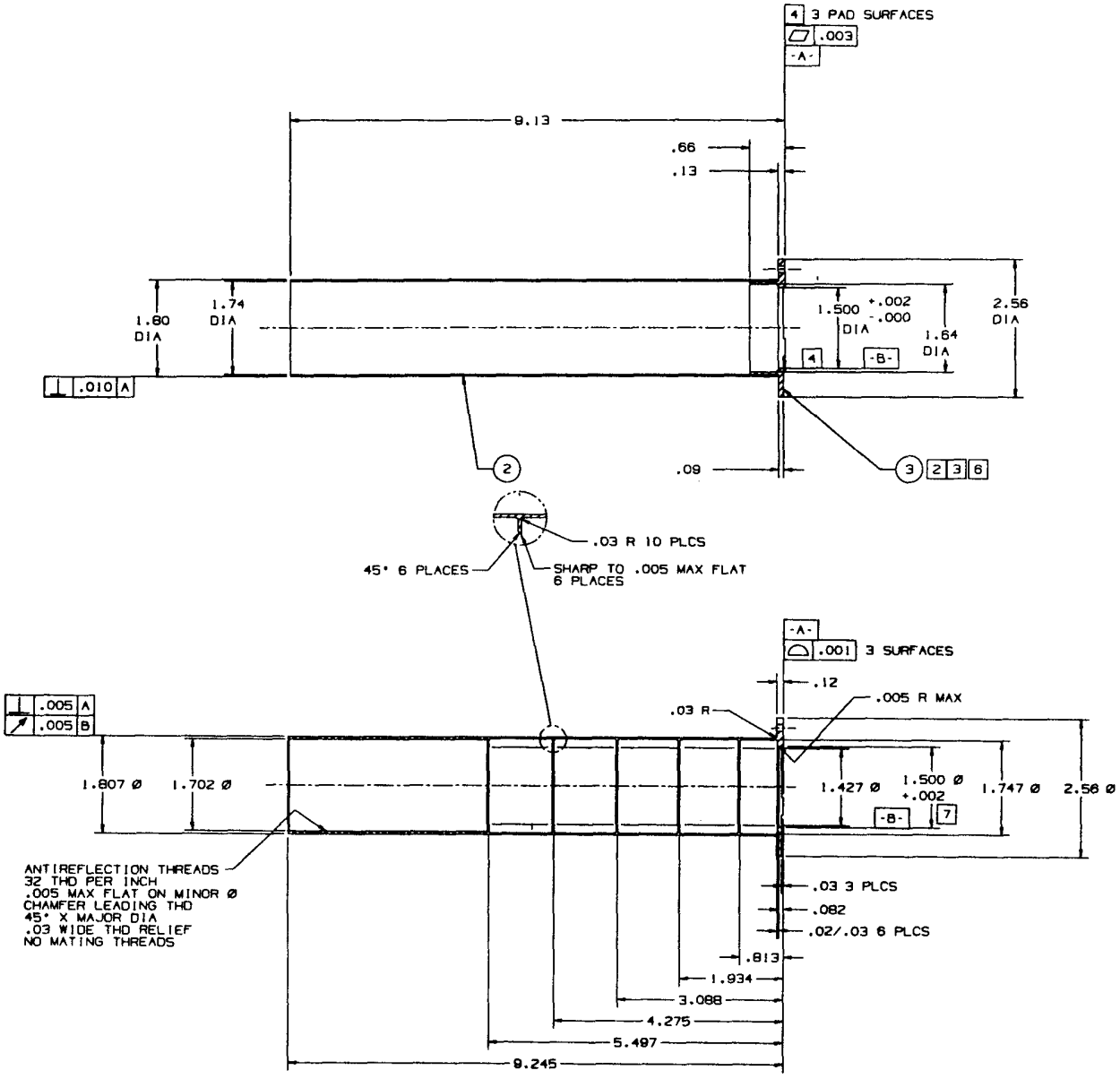

Figure 2.2. Original Light Shield design (a) and revised Light Shield design (b).

3. VIBRATION TESTING

Vibration testing with the MOC Engineering Model (EM) was useful in validating the initial design, because design weaknesses were able to be detected and changed early in the design process. After making design changes to the primary mirror mount, secondary mirror mount, and MBSA facesheets, the EM eventually passed at Proto-Flight (PF) levels with no failures. Although a significant amount of vibration testing had been performed on the EM, no vibration testing had been done on the Flight Unit #1 until August 1990.

3.1 August 1990 vibration testing

The first vibration testing done on Flight Unit #1 was performed to the Proto-Flight (PF) levels shown in Figure 3.1. As with the EM, testing was done with a T-1000 shaker and a test fixture base rigid enough to avoid introducing its own resonances (solid aluminum, 18 inches in diameter by 2 inches thick). Although the purpose of this testing is only to ensure that the unit will pass without damage, a 3-axis response accelerometer was affixed to the Wide-Angle Transition Bracket to check loading in that area.

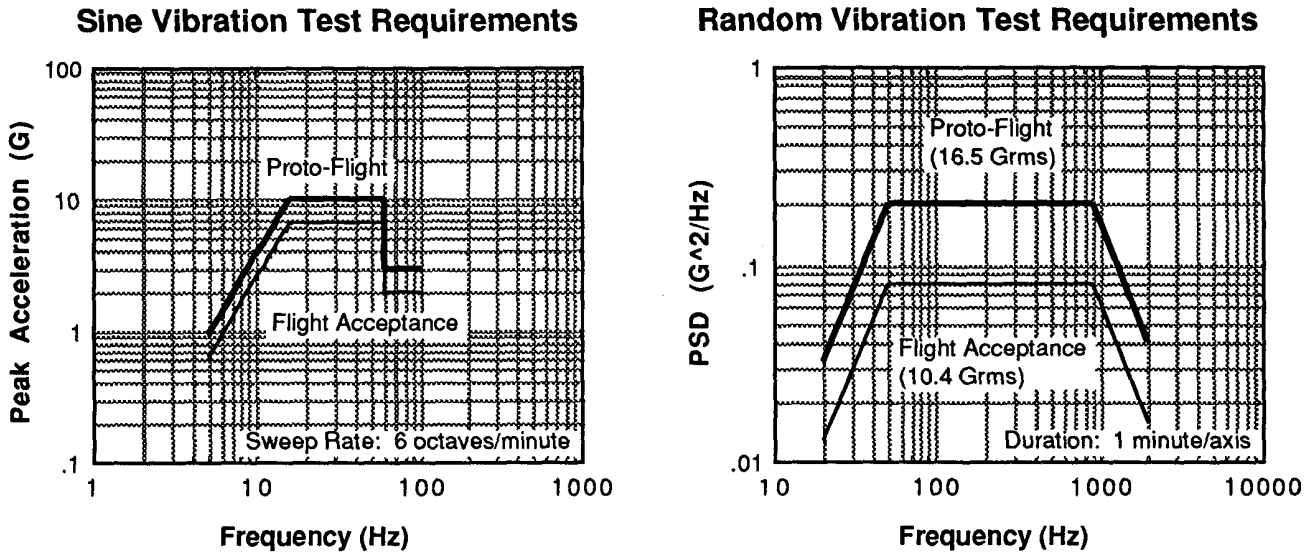

Figure 3.1. Sine vibration test requirements (a) and random vibration test requirements (b) for Mars Observer Spacecraft nadir panel-mounted instruments.

The unit successfully passed the sine vibration test; however it sustained some damage during random vibration testing. After the first run (x-axis, perpendicular to the Wide-Angle Baffle) we noticed two broken epoxy bonds on the metering structure. The outermost stiffening/baffle ring became detached from the main tube approximately one-third of its perimeter, and the next ring down detached approximately one-sixth of its perimeter. At the time of test it was decided that these failures would not cause further damage if testing continued. Therefore, testing was resumed to see if other parts of the structure also had latent weaknesses. The unit survived without further damage.

Standard procedure requires an interferometric check to ensure that the primary-to-secondary alignment is not disturbed by vibration testing. On performing this routine check, approximately 1.5 waves of coma were observed. (.0045 inches secondary mirror decenter will produce 1.5 waves of coma at $\lambda = 632.8$ nm.) It was also noticed that by pushing or pulling radially on the spider vanes, tilt could be introduced and the interferometric pattern would take on a new set. The secondary mirror could be tilted and assume a set at angles up to 46 μrad (4 waves). Upon closer inspection, we noticed that the bond fillets where the spider vane tenons engage the metering structure tube mortises had fractured as well.

After machining a .63 x 1.45-inch access hole in the metering structure tube to inspect inside the closed-out spider stiffening annulus, the cause of the problem became clear. The bonding of the spider vanes to the lower ring was incomplete according to the original design. To reinforce the area and mend the inspection hole, doublers were bonded to either side of each spider vane and each inspection cutout was patched. A backlock was bonded between each pair of doublers as they protruded from the metering structure tube (see Figure 3.2). After repairing the outer two stiffening/baffle rings with thicker bond fillets, Flight Unit #1 was ready for its second attempt at PF random vibration testing.

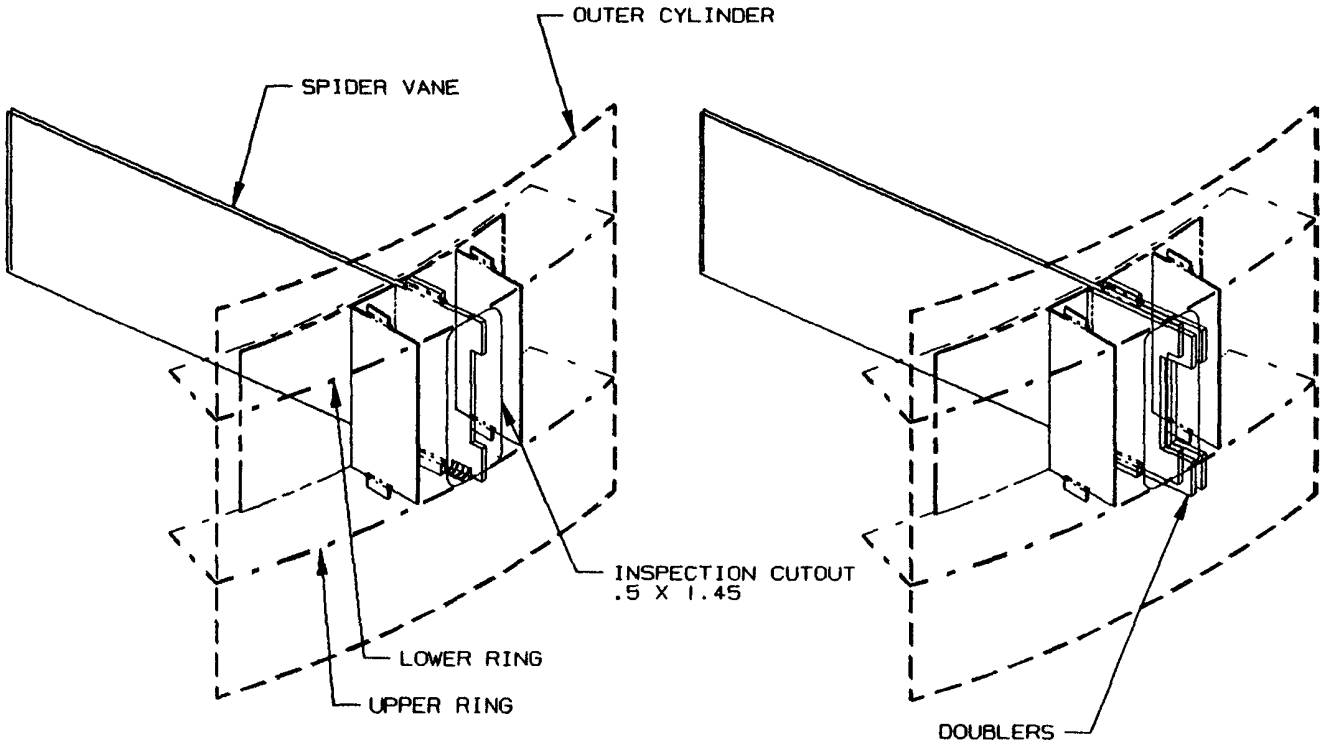

Figure 3.2. Spider stiffening annulus inspection and repair.

3.2 January 1991 vibration testing

After Flight Unit #1 sustained damage during vibration testing, the required load levels were re-examined. It was determined that the specified load levels at the nadir panel, in actuality, would not be fully imparted to the MOC because the nadir panel is not infinitely rigid and will absorb some energy, particularly at MOC resonant frequencies. Terry Scharton of JPL developed a test plan that would vibration test the MOC unit at PF levels, but limit the force imparted to the unit as though the vibration spectrum were being delivered by the nadir panel[3,4]. This force limiting technique is summarized in Figure 3.3.

The amount of force limiting is dependent upon the nadir panel effective mass, which is a function of frequency. The effective mass of the nadir panel was measured using a modal impact hammer, and data was obtained at each of the three MOC attach points and in each axis. The total nadir panel effective mass for each axis was assumed to be the sum of the effective masses at each attach point. The total nadir panel effective mass ranged from 83 lbs at 25 Hz (y-axis) to 3 lbs at 800 Hz (z-axis, nadir pointing).

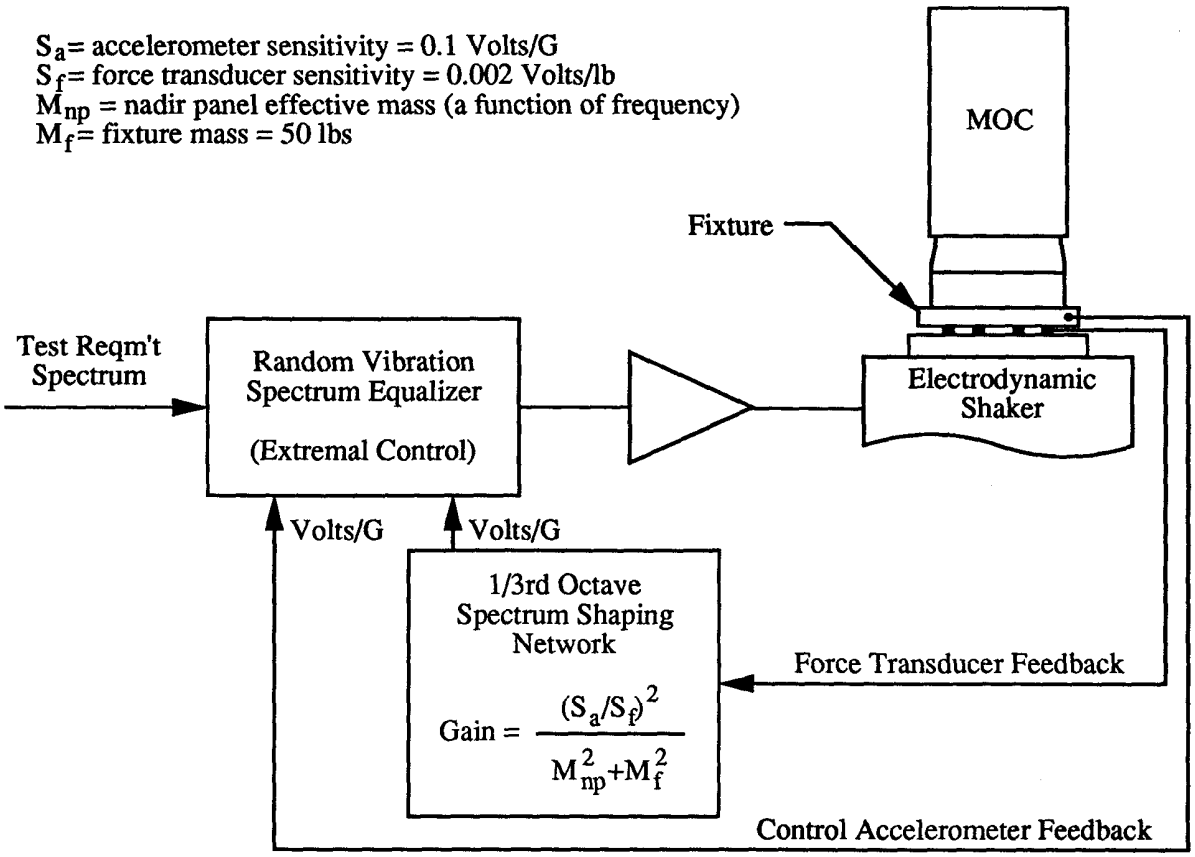

Figure 3.3. Force limiting control loop.

This test was conducted more analytically and cautiously in case there should be another problem. The MOC unit was outfitted with six tri-ax response accelerometers attached in critical locations, and another finite element analysis was run to predict the RMS and 3σ G-levels at these locations for the specified random vibration spectrum. The predicted 3σ G-levels were incorporated as test limits such that the test would automatically terminate if any one of these levels was exceeded. The test sequence for vibration testing in each axis was as follows:

1. 0.5 G sine survey of the MOC and fixture to obtain baseline response (10-2000 Hz)
2. PF spectrum -12 dB to gather data for force limiting corrections (30 second duration)
3. PF spectrum -12 dB with force limiting, to ensure no problems (30 second duration)
4. PF spectrum -6 dB with force limiting, to ensure no problems (30 second duration)
5. PF spectrum with force limiting (actual test, 60 second duration)
6. 0.5 G sine survey of the MOC and fixture to compare with baseline to ensure no changes (10-2000 Hz)

At the time of test, the z-axis sequence was changed to take force limiting data at the PF spectrum -18 dB, and run checks at -18, -12, and -6 dB with force limiting, before testing at the full PF spectrum with force limiting.

Flight Unit #1 passed this vibration test without damage, but not without incident. The z-axis PF spectrum -6 dB test was attempted three times, but kept terminating because the G-level limit set for the Transition Bracket location (13 G at -6 dB) was exceeded (38 G @ 1 sec, 65 G @ 3 sec, and 70 G @ 13 sec). Further force limiting was employed by notching the spectrum at 300, 400, and 600 Hz. This time the PF spectrum -6 dB test ran to completion, but with the same force limiting, the full PF spectrum test terminated after 2 seconds (75 G at the Transition Bracket exceeded the 53 G limit). Since no further force limiting could be justified, the Transition Bracket G-level limit was set at 100 G, and the test completed successfully.

4. THERMAL EXPANSION TESTING

In order to be able to predict the axial displacement of the telescope image plane with temperature, the relative axial motions of the primary and secondary mirrors must be determined. From early testing of the MOC EM, it was discovered that there were two other thermally-driven mechanisms associated with the MOC graphite/epoxy structure, besides the metering tube, that governed the relative displacement of the primary and secondary mirrors. It was found that the spider has a slight motion with temperature causing the secondary mirror mounting surface to shift axially relative to the intersection of the spider with the metering tube, and the base has a slight motion such that the primary mirror mounting surface shifts axially relative to the attach points at the base of the metering tube.

4.1 Test procedure

Composite Optics, Inc. (COI, San Diego, CA) performed thermal expansion tests on both Flight Units to measure each of these thermally-driven motions. Their test method utilized the dilatometer set-up shown in Figure 4.1. A HeNe laser beam is directed onto a partially transmissive tilt mirror, which is supported on one end by a reference standard of precisely known, or zero, CTE, and on the other end by the test article. The relative motions of the test sample and reference standard can be determined by the changes in the relative spacings of the spots projected onto a remote screen by the multiple reflections between the tilt mirror and the polished end of the reference standard. The purpose of the evacuated column is to minimize the path length of turbulent dry nitrogen, that can limit the accuracy of the spot measurements.

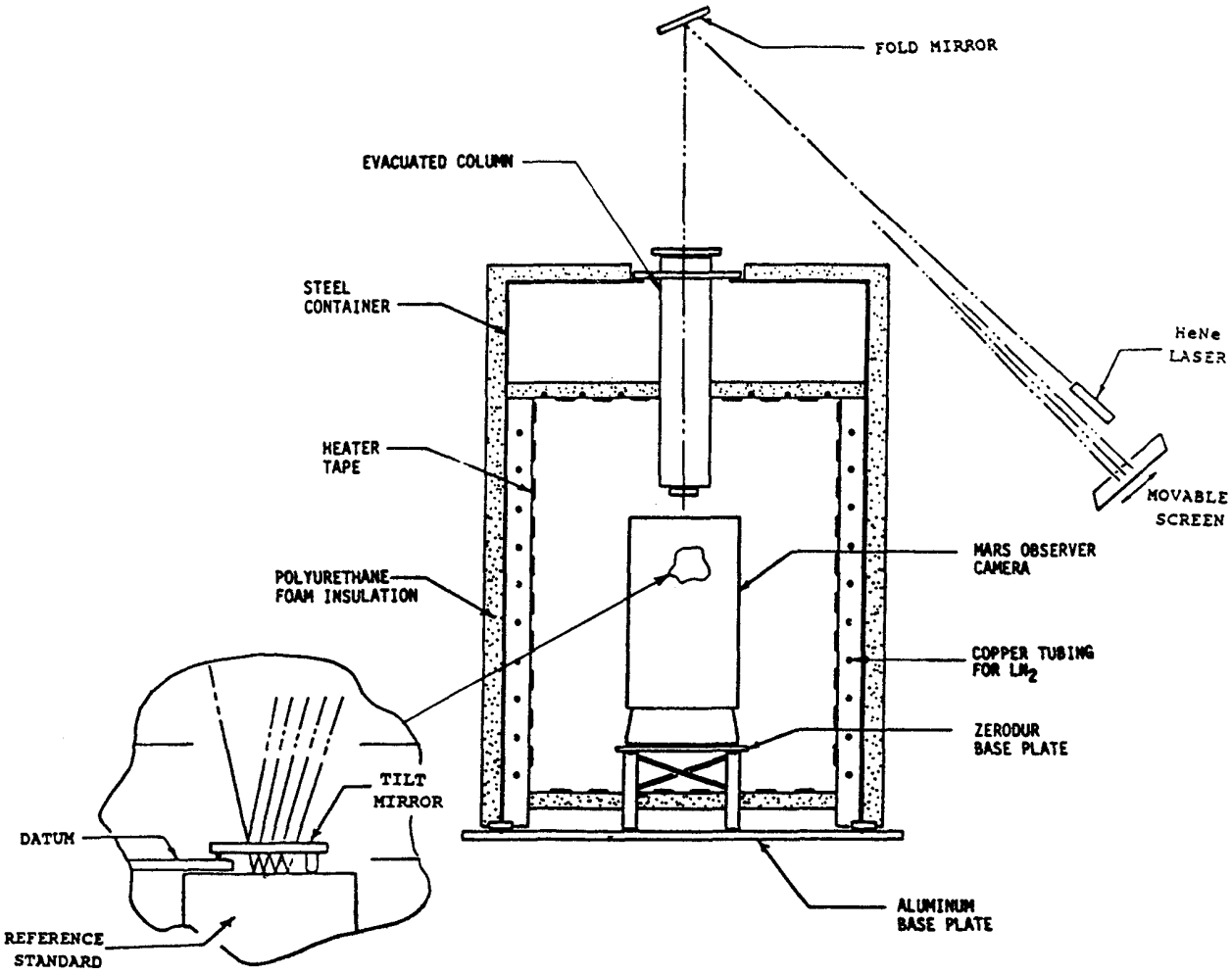

Figure 4.1. COI thermal expansion dilatometer set-up.

The ΔL (as a function of T) must be determined for each contributor individually because the base, metering tube, and spider are never at the same temperature during operation. Only the ΔL/L(T) of the metering tube can be measured directly (as shown in Figure 4.2a). The ΔL(T) of the base must be determined by measuring the ΔL(T) between the primary mirror mounting surface and the top of the metering tube (shown in Figure 4.2b), and subtracting the ΔL(T) due to the metering tube. The ΔL(T) of the spider is determined by measuring the ΔL(T) between the primary mirror mounting surface and the secondary mirror mounting surface (shown in Figure 4.2c), and subtracting the ΔL(T) due to the base and the applicable length of metering tube.

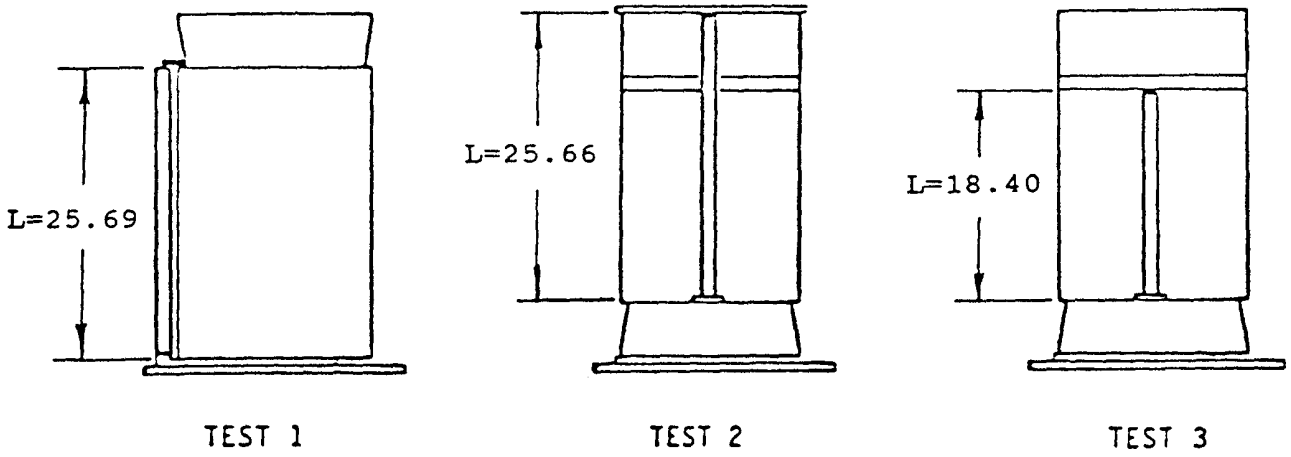

Figure 4.2. Test configurations to derive the ΔL(T) of the tube (a), the base (b), and the spider (c).

Since at the time of test, the depth of focus of the telescope was assumed to be approximately ±.002 inches (the allowable depth of focus was later determined to be ±.00465 inches), and the axial magnification of the telescope is approximately 56, the net ΔL(T) from all three contributors had to be determined to an accuracy of better than ±36 μinches. The goal was to measure ΔL/L(T) to better than 1 ppm in each test configuration. The existing test set-up needed to be refined to achieve this accuracy. The experience of Professor Steve Jacobs of the University of Arizona was called upon to determine ways in which this level of accuracy could be achieved. The following improvements (in no particular order) were implemented, and the accuracy and repeatability in measurements significantly improved (the uncertainty in each data point was on the order of 0.5 ppm; however, the repeatability/hysteresis was on the order of 2 to 3 ppm).

1. The test environment must not cause the graphite/epoxy structure to absorb or desorb moisture during testing, otherwise the moisture-induced length change is perceived as a temperature-induced length change. Therefore, the structure must be thoroughly baked-out in situ in a dry nitrogen environment, and the dry nitrogen environment maintained during testing.
2. The data should be taken after the *motion* has stabilized at the desired temperature, not after the desired *temperature* has stabilized.
3. The baseplate should be made from a thermally stable glass, such as Zerodur, and should be thermally cycled before using in test.
4. The baseplate should be insulated from the concrete floor to limit thermal gradients in the baseplate that might cause warpage.
5. If the standards are to be made from Zerodur, they should be maintained at a constant temperature throughout testing (with heaters and insulation) because Zerodur exhibits hysteresis. ULE and Cer-Vit (Cer-Vit is no longer manufactured) exhibit no hysteresis.
6. All exposed glass reference surfaces should be stress relieved by either polishing or acid etching to avoid warping with temperature.
7. The liquid nitrogen should be completely vaporized before introduction into the test chamber and the circulation fan should be situated such that it does not influence the tilt mirror.
8. Vibration to the glass baseplate should be reduced as much as possible to avoid upsetting the tilt mirror.

9. The kinematic points on the tilt mirror should not be overconstrained by the surface roughness of the reference standard or test article.

4.2 Test results

After measuring ΔL as a function of temperature for each test configuration, the individual motions of the base, tube, and spider can be derived. Figure 4.3 shows the derived primary-to-secondary mirror mounting surface spacing change due to the temperature of each of the individual contributors. A negative value means that the spacing is shortened; a positive value means the spacing has increased. To elucidate, as Flight Unit #1 goes cold, the primary mirror mounting surface moves up towards the secondary mirror, the spider moves up (away from the primary mirror), and the metering tube shrinks. As Flight Unit #2 goes cold, the primary mirror mounting surface moves down (away from the secondary mirror), the spider moves ever so slightly upward (away from the primary mirror), and the metering tube grows.

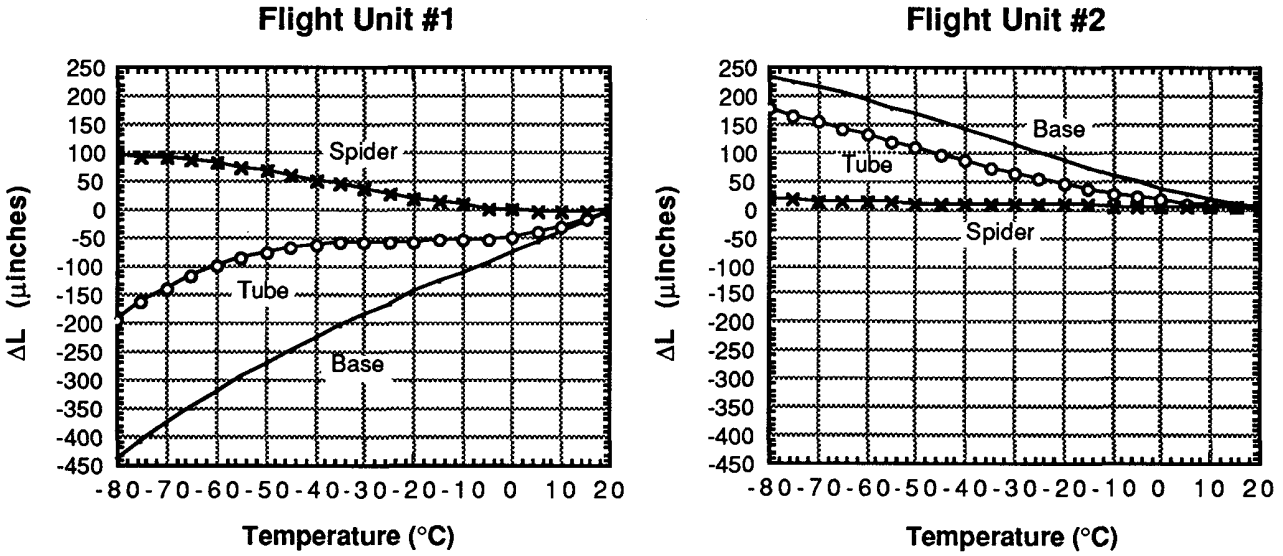

Figure 4.3. Relative displacements between the primary and secondary mirror mounting surfaces of the Flight Unit #1 (a) and Flight Unit #2 (b) graphite/epoxy structures.

The negative CTE of the Flight Unit #2 metering tube was attributed to its higher average fiber volume content (and the fact that the Flight Unit #1 metering structure has MH21S/LO painted on its interior may contribute further to its positive CTE). The thermally-driven mechanism that causes the spider and base to deflect is unclear. It is speculated that perhaps the spider deflects due to the expansion or contraction of the metering tube around it, and the base deflects due to the differential expansion between its graphite/epoxy structure and Invar fittings.

Although these thermal expansion tests were run from room temperature to -115°F (-81.7°C), recent thermal analysis (taking the internal MLI blanketing into account) has shown that during operation, the MOC unit will only experience the temperatures shown in Table 4.1.

	Aphelion	Perihelion
Spider	-51°C	-31°C
Tube	-51 to -45°C	-31 to -25°C
Base	-41°C	-21°C

Table 4.1. MOC operational temperatures.

5. THERMAL-VACUUM TESTING

Based on the relative progress and the characterization of the two flight units, it was decided that Flight Unit #1 would be the unit to be launched. From February to May 1991, thermal-vac testing was performed on Flight Unit #1. The purpose of thermal-vac testing was threefold:

1. To check the image plane displacement from its room temperature location to its operational location (to be able to accurately set the focal plane such that the camera will be in focus during operation in Martian orbit).
2. To check that the image plane excursion between operational scenario extremes does not exceed the telescope's depth of focus (since there is no active focus control).
3. To ensure that the operational environment does not cause the optics or structure to deform in such a way to cause aberrations.

5.1 Method

The method used to meet these objectives involved integrating an interferometer with a thermal-vac chamber. The MOC axial focal point displacements were measured interferometrically for each temperature scenario using a reference sphere and a return flat (see Figure 5.1). A reference reticle was implemented to provide a reference point for alignment and taking measurements. The temperature scenarios were achieved with the 77K and vacuum environment provided by the thermal-vac chamber, and the thermal loads provided by various MOC heaters. The MOC unit had to be baked-out prior to testing (as it will be by the time it reaches Mars) to remove all moisture that could be desorbed during test, resulting in spurious results. A majority of the bake-out (2 weeks) was performed in a smaller chamber to avoid the high cost of running the large thermal-vac chamber; but the final bake-out (3 days) had to be performed in the test chamber to remove the small amount of moisture absorbed during transfer from chamber to chamber.

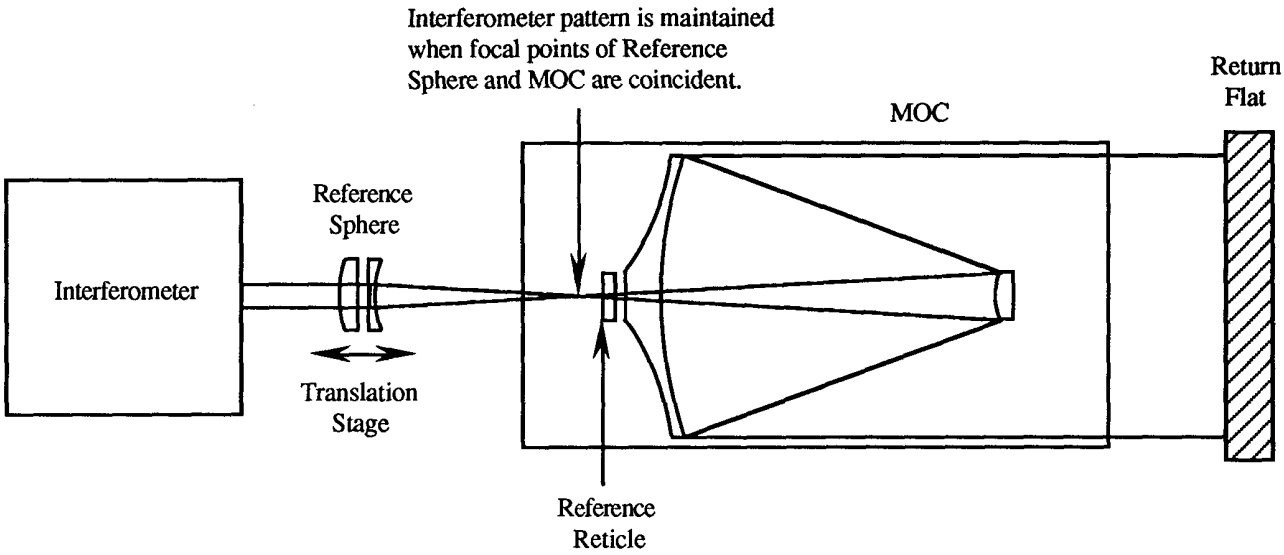

Figure 5.1. MOC interferometric test set up. MOC axial focal point displacements can be measured directly by the reference sphere displacement required to regain the interferometric pattern.

5.2 Test set-up

An available thermal-vac chamber that met our inside dimension and view port requirements was located at TRW (Redondo Beach, CA). The necessary test bench and support fixturing was designed to and assembled into this chamber (see Figure 5.2). The vibrational stability of the path length between the reference sphere and return flat is critical, so it was necessary to

design extremely rigid fixturing. The reference sphere translation stage was fixed externally to the thermal-vac chamber view port flange, the MOC support fixture was internally fixed to the view port flange, and the MOC support fixture was fixed to the return flat mount with an aluminum truss structure. A special vibration-suppression mount was designed to hold the return flat. (We learned that cadmium-plated or non-stainless steel fasteners should not be used in thermal-vac. The cadmium plating outgases in vacuum, and non-stainless steel can fracture at temperatures below ≈-150°F (172K)).

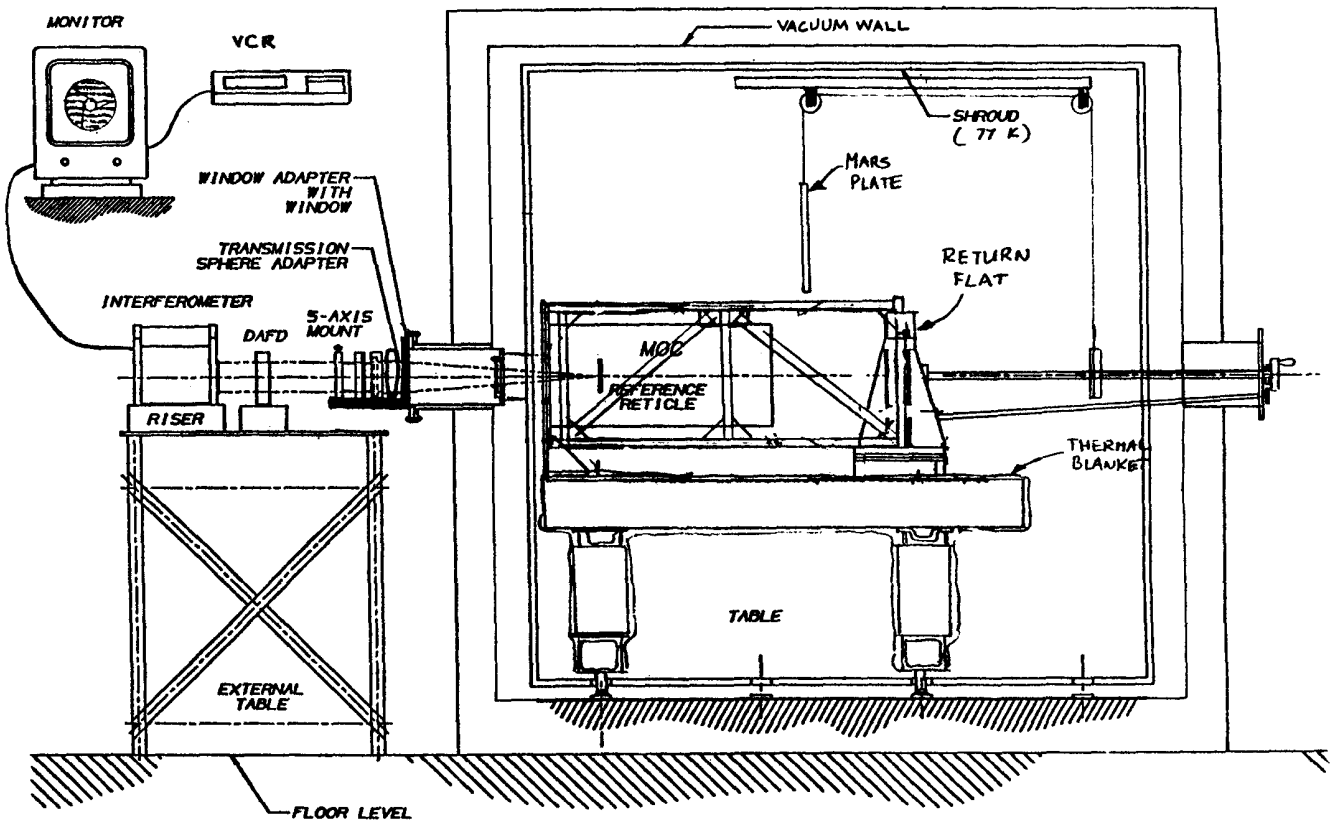

Figure 5.2. MOC thermal-vac test set-up.

Due to the size of the view ports, the return flat had to be placed inside the chamber. The alignment of the return flat is lost when the chamber is evacuated and between different temperature scenarios. To still be able to adjust the tip and tilt of the return flat from outside the chamber, extension rods with wafer spring couplings on both ends were designed to connect the return flat mount adjustments to ferrofluidic feedthru knobs on the opposing port plate. The return flat substrate material is Zerodur, and although Zerodur is thermally very stable, there was concern that the surface flatness may change with temperature. A full aperture interferometric test could not be performed on the return flat alone because the view ports were too small and the maximum interferometer beam diameter was 4 inches. To check the mirror's flatness at 77K, a "skip test" was performed. The return flat was set in the chamber such that the 4-inch interferometer beam grazed the surface and spanned the return flat's 16-inch diameter. The beam was returned back on itself by a 4-inch diameter flat external to the chamber at the opposite view port. At least over this 4 x 16-inch swath, the return flat remained flat at 77K.

Various heaters were used to simulate the heat loads the MOC would experience in Martian orbit. The actual sources of heat to the MOC will be from the sun, Mars, the spacecraft, and MOC internal electronics. These heat loads were simulated by

the following:

1. Solar and spacecraft radiation -- 12 Kapton-film patch heaters were placed on the metering tube (4 around the periphery, at the upper third, center third, and lower third of its length) under the external MLI blanketing. 2 patch heaters were placed around the periphery of the aluminum Base Radiator. These heaters were powered as necessary to yield the temperature profile determined from the thermal analysis.
2. Martian radiation -- Radiation from Mars was simulated by a black-anodized aluminum plate supported directly in front of the MOC, which had a strip heater attached to its rear surface, and MLI over that (to make the heaters more efficient and prevent warming the return flat). The "Mars plate" was controlled to -30°C for nominal perihelion conditions, and -53°C for nominal aphelion conditions. The Mars plate was on a pulley system such that it could be retracted just prior to making an interferometric measurement.
3. Spacecraft conduction -- Patch heaters were placed on the "nadir panel simulator" by each MOC attach point and warmed to the appropriate degree depending on the scenario.
4. Internal electronics -- The three electronics board mass models used in vibration testing performed double-duty. A hole had to be bored through the center of each board to allow the light to pass for interferometric testing. Resistors were bonded to each board to yield the appropriate distribution of wattage, and the boards were painted with a black paint that would mimic the emissivity of the conformal coating to be applied to the actual boards. The resistors on the top and bottom surface of the uppermost board (the analog board) were nominally powered at 0.3 W each surface. The resistors on the center board (the upper digital board) were nominally powered at 4.6 W. The resistors on the lowermost board (the lower digital board) were not powered, as this board in actuality is a spare, and no testing was done assuming the spare is activated.

Naturally, the temperature of any single location on the MOC is affected by some combination of these heaters, so the heaters that could be powered to a predetermined level (the internal electronics and the Mars plate) were powered to that level, and the remainder of the heaters were powered as necessary to obtain the desired temperature profile determined from the thermal analysis.

5.3 Test scenarios

MOC focal point displacements were measured at 7 different thermal cases (see Table 5.1). Only two of the cases (cases 1 and 6) were actual nominal conditions. The other cases were experiments to see what effect certain heat load perturbations would have on the temperature profile and resulting image displacement (in case our assumptions about the actual conditions were off).

Case		Base Radiator Temp (°C)	Electronics Board Loads (W)			Nadir Panel Temp (°C)	Mars Plate Temp (°C)
			Top Analog	Bottom Analog	Upper Digital		
1	**Perihelion, 1.797 hours (max nominal temperature case)**	0	0.3	0.3	4.6	18	-30
2	Case 1, with Base Radiator temp perturbed +15°C	15	0.3	0.3	4.6	18	-30
3	Case 1, with Electronics Board loads perturbed +25%	0	0.4	0.4	5.8	18	-30
4	Case 1, with Nadir Panel temp perturbed +10°C	0	0.3	0.3	4.6	28	-30
5	Case 1, with Mars Plate temp perturbed +15°C	0	0.3	0.3	4.6	18	-15
6	**Aphelion, 0.95 hours (min nominal temperature case)**	-16	0.3	0.3	4.6	3	-53
7	Case 6, with Base Radiator temp perturbed -15°C	-31	0.3	0.3	4.6	3	-53

Table 5.1. Thermal-vac test temperature scenarios. Cross-hatched values represent temperatures that were not controlled. The heaters that control these temperatures were fixed at the wattages determined from the nominal cases.

5.4 Test results

In areas on the MOC where there was no heater control, yet thermocouples to sense the temperature (e.g., the primary mirror), the temperature was on the average within 1°C of the temperature predicted by the thermal analysis; thereby bolstering faith in the thermal analysis and our ability to simulate Martian orbit conditions. It was also found that the differences in temperature profile and resulting image displacement caused by the perturbation cases were very small in comparison to the differences between the nominal perihelion case and the nominal aphelion case.

However, based on the temperature profiles collected from the thermal cases and our understanding of the thermally-driven optics and structure changes, we expected to see focal point displacements (from room temperature location) on the order of -.010 inches for the perihelion cases, and roughly -.017 inches for the aphelion cases (a negative value means the focus shifts shorter). Instead, we measured focal point displacements on the order of -.036 inches for the perihelion cases, and roughly -.051 inches for the aphelion cases. Experts from JPL, Caltech, OCA Applied Optics, COI, and Ball Aerospace were unable to explain the discrepancy after a thorough review of the test set-up and the separate thermal expansion data of the optics and structure.

It should be noted that room vibrations made the interferometric measurements very difficult. Even with the cryo-pump turned off, there was a significant amount of residual vibration. Several displacement measurements were taken at each thermal case and the resulting 1σ error in the displacement from room temperature for each thermal case was on the average .005 inches.

Although the room vibrations made the displacement measurements difficult, we were still able to measure the wavefront quality. A VCR was used to record the video image from the interferometer, and when played back in slow motion, certain frames could be found where the interferometric image was stable for that instant. From this, it was determined that the thermal environment does not impact the image quality. Unfortunately, this technique could not be used to reduce the uncertainty in the displacement measurements, as it is very time consuming, and there is only a few minutes that the cryo-pump can be turned off (air begins to leak past the head gate) and the Mars plate can be retracted (the end of the MOC begins to cool).

5.5 Thermal-vac test conclusions

1. Measured nominal temperature profiles were very close to expected.
2. Thermal perturbations representing a gross uncertainty in the actual environment have little effect on the temperature profile and resulting image displacement.
3. Unable to account for ($\approx$ factor of 3) difference between expected and measured focal point displacements from room temperature location.
4. Thermal environment does not impact image quality.

The focal plane will be set approximately .044 inches inward of its room temperature best focus location, such that it will lie halfway between the measured aphelion and perihelion displacements when in Martian orbit. However, since the measured focal point displacements between aphelion and perihelion exceed the depth of focus of the telescope (.051-.036 = .015 inches), a method of active focus must be employed.

Since the most sensitive part of the telescope to thermally-induced defocus is the primary mirror, a scheme to keep the camera focused to within its depth of focus was developed based on warming the primary mirror with rim and hub heaters. This technique is explained in "The effects of thermal gradients on the Mars Observer Camera primary mirror"[5].

6. ACKNOWLEDGMENTS

The accomplishments reported in this paper summarize a team effort, with many vital contributions made by employees of Caltech, Altadena Instruments, OCA Applied Optics, and Composite Optics, Inc. Credit for successes and achievements of the Mars Observer Camera are rightfully shared with these individuals and groups. The author (OCA MOC Project Engineer) is simply the necessarily singular channel through which this team has communicated these efforts.

The author particularly wishes to thank Col. David R. Hughes, USAF (Ret.), OCA MOC Program Manager, for the encouragement for this paper to be written. The author also wishes to thank Dr. Michael C. Malin, the MOC Principal Investigator, and Dr. G. Edward Danielson, the MOC Instrument Manager, for their support. The author is once again indebted to Mr. Michael A. Ravine, MOC Deputy Instrument Manager, Mr. Lawrence J. Steimle, and the folks at Composite Optics, Inc., for their technical assistance (helping me keep the facts straight).

7. REFERENCES

1. "The Mars Observer", JPL 410-30, Issue 5, Jan. 1992.
2. A. R. Telkamp and E. A. Derby, "Design considerations for composite materials used in the Mars Observer Camera", SPIE Vol. 1303 Advances in Optical Structure Systems, pp. 416-436, Orlando, April 1990.
3. T. Scharton, "Force Specifications for Extremal Dual Controlled Vibration Tests", 61st Shock and Vibration Symposium, Pasadena, CA, 1990.
4. T. Scharton, D. Boatman, and D. Kern, "Dual Control Vibration Testing", 60th Shock and Vibration Symposium, Virginia Beach, VA, 1989.
5. R. W. Applewhite and A. R. Telkamp, "The effects of thermal gradients on the Mars Observer Camera primary mirror", SPIE conference 1690 Design of Optical Instruments, paper 45, Orlando, April 1992.